J Math Chem (2012) 50:805–818
DOI 10.1007/s10910-011-9925-1

ORIGINAL PAPER

The analytical determination of kinetic parameters for a bimolecular EC mechanism from chronoamperometric data

K. T. Gimre · R. V. Whiteley Jr. · C. M. Guenther

Received: 22 July 2011 / Accepted: 30 September 2011 / Published online: 15 October 2011

Abstract We study the dependence of chronoamperometric data on the kinetic parameters for a bimolecular reaction, characterizing the behavior of an electrochemical mechanism that pertains to lithium/sulfur dioxide batteries. The reaction entails first the reduction of a reactant O to a product R by an instantaneous charge transfer, followed by a homogeneous chemical reaction between O and R to produce an electrochemically inert product P. We model this by a semilinear reaction-diffusion system with discontinuous initial conditions and mixed Dirichlet and Neumann boundary conditions, and develop a procedure to extract from a single potential step experiment the forward and reverse rate constants for the reaction. To do so we define a function $\mathcal{J}(t) := j(t)\sqrt{t}$, where $j(t)$ is the current density from the chronoamperometric output, and use maximum principle and scaling arguments to exploit the location of the minimum of $\mathcal{J}(t)$ versus t.

Keywords Chronoamperometry · Chemical kinetics · Inverse problems · Semilinear reaction-diffusion systems

K. T. Gimre
Department of Mathematics, Columbia University, New York City, NY, USA

R. V. Whiteley Jr.
Department of Chemistry, Pacific University, Forest Grove, OR, USA

C. M. Guenther (✉)
Department of Mathematics and Computer Science, Pacific University, Forest Grove, OR, USA
e-mail: guenther@pacificu.edu

1 Introduction

The use of potential step chronoamperometry and chronocoulometry for the characterization of chemical reactions that follow an instantaneous charge transfer reaction (the EC mechanism)

$$O + ne^- \rightleftharpoons R \tag{1}$$

has been described for several types of reactions (Reactions 2–5). There is the first order decay of the reduction product, R, to produce an electrochemically inactive product, P (Eq. 2) [1–3],

$$R \rightarrow P \tag{2}$$

and there are several follow-on reactions which lead to regeneration of O, the electrochemical reactant, which are either first [4,5] or second order [4] in R. (In Reaction 3, S is an electrochemically inactive reactant.)

$$R + S \rightarrow O + P \tag{3}$$
$$R + R \rightarrow O + P \tag{4}$$

Another such second order reaction, the dimerization of R has also been studied using a double potential step method [6].

$$R + R \rightarrow P \tag{5}$$

The dimerization has particular relevance to the cathodic half-reaction of the Li/SO_2 battery wherein the SO_2 is reduced to the SO_2^{1-} free radical which then dimerizes to the dithionite ion, $S_2O_4^{2-}$ [7]. But also relevant to the Li/SO_2 battery is an alternative follow-on reaction in which the SO_2^{1-} reduction product reacts with SO_2 to form the $S_2O_4^{1-}$ adduct [8,9]. In terms of Reactions 2–5, this can be expressed as

$$R + O \underset{k_b}{\overset{k_f}{\rightleftharpoons}} P. \tag{6}$$

Note that we write this more generally than Reactions 2–5, allowing that this follow on reaction can run forward at a rate k_f or backwards at a rate k_b.

Reaction 6 looks like a simple complement to Reaction 3, because here R consumes rather than generates O. However, the theoretical treatment of Reaction 3 has been for a heterogeneous reaction between R and S which is taken to be zero order in S, resulting in a linear system of differential equations. Reaction 6, however, must be modeled by a semilinear system, and so linear techniques such as the Laplace transform method no longer apply, and even short term existence and uniqueness are not a priori known. Further complications include mixed Dirichlet and Neumann boundary conditions, discontinuous initial conditions, and an infinite spatial domain.

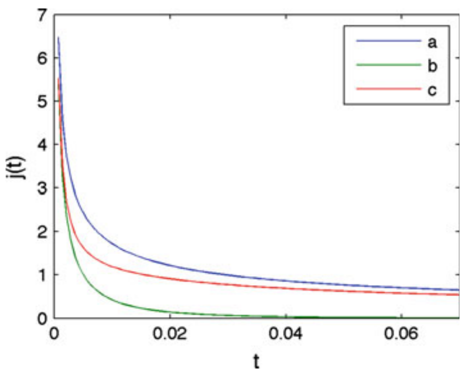

Fig. 1 Chronoamperometric response (expressed in current density $j(t)$) for three kinetic conditions with $C_b = 10^{-3}$ mol $\cdot$ cm^{-3} and $D_O = D_R = 2D_P = 10^{-5}$ cm$^2 \cdot$ s^{-1}; k_f is in cm$^3 \cdot$ mol$^{-1} \cdot$ s^{-1} and k_b is in s^{-1}. Curve 'a' corresponds to $k_f = k_b = 0$, 'b' to $k_f = 10^6$, $k_b = 0$, and 'c' to $k_f = 10^6$, $k_b = 250$

We take the reaction between R and O as a homogeneous, bimolecular reaction which is first order in R and O with forward and reverse rate constants k_f and k_b, respectively. The experiment is begun with C_b as the initial concentration of O. As in all studies cited here, we take the potential step to cause an effectively instantaneous charge transfer and to be sufficiently large to drive the concentration of O at the electrode surface to zero and create diffusion controlled mass transport of O to the electrode and R from the electrode.

Our goal is to deduce the rate constants from a single potential step experiment from chronoamperometric data, $j(t)$, governed by

$$j(t) = nFD_O \left.\frac{\partial O}{\partial x}\right|_{x=0}. \tag{7}$$

Here n is the number of electrons transferred to O in the electrochemical reaction; F is Faraday's constant; D_O is the diffusion coefficient of O; O is the concentration of O; and $\frac{\partial O}{\partial x}$ is the concentration gradient of O, with x the distance from the electrode. All concentrations are molar concentrations.

The problem is that most current density curves look essentially the same. For example a family of plots of $j(t)$ versus t is shown in Fig. 1. Here, $j(t)$ is in amp $\cdot$ cm^{-2}.

Without prior knowledge of the rate constants that produced the three curves in Fig. 1, there is such small variation between the curves that it would be difficult to differentiate between them. However, the rate constants that produced the curves are significantly different: for one, 'a', both rate constants are zero, for the second, 'b', $k_f = 10^6$ and $k_b = 0$, and for the third, 'c', $k_f = 10^6$ and $k_b = 250$.

There are, however, certain distinctions between the curves that we can exploit to simplify calculations and accentuate differences. We introduce here a novel way of presenting chronoamperometric data, $j(t)$, that *immediately* differentiates between the cases $k_f > 0$ and $k_f = 0$, and $k_b = 0$ and $k_b > 0$. We define a function

$$\mathcal{J}(t) := j(t)\sqrt{t},$$

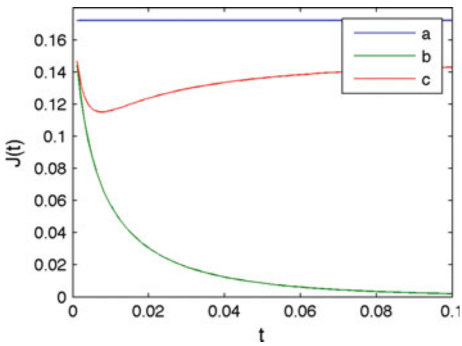

Fig. 2 Normalized chronoamperometric response (expressed as normalized current density $\mathcal{J}(t)$ in amp $\cdot$ s$^{1/2}$ $\cdot$ cm^{-2}) for the same three kinetic parameters, C_b, and diffusion coefficients of Fig. 1

and consider the plot $\mathcal{J}(t)$ versus t. Recall that a charge transfer that is not followed by a chemical reaction must have $k_f = 0$ and so $j(t)$ is given by the Cottrell equation,

$$j(t) = nFC_b\sqrt{\frac{D_O}{\pi t}} \tag{8}$$

[11]. Therefore, $\mathcal{J}(t)$ will be manifest as the constant $nFC_b\sqrt{\frac{D_O}{\pi}}$ for all t. It is shown[1] in Fig. 2 (and proven in Sect. 3) that because the consumption of incoming O by outgoing R will mitigate the supply of O to the electrode, $\mathcal{J}(t)$ must deviate more and more negatively from the constant with increasing k_f.

Moreover, it is shown in Fig. 2c and proven in Sect. 3 that when k_f and k_b are positive there exists a minimum of $\mathcal{J}(t)$. In Sect. 4 we use scaling and maximum principle arguments to determine $\frac{k_f}{k_b}$ from the value of this minimum. From the coordinates of the minimum, we then find k_b. When $k_f > 0$ but $k_b = 0$, there is no such minimum as shown in Fig. 2b, but k_f can, nevertheless be calculated from the deviation of $\mathcal{J}(t)$ from $k_f = 0$ behavior. This also is described and illustrated in Sect. 4.

1.1 Outline

The outline of the paper is as follows: in Sect. 2 we model the reaction by an initial boundary value system of semilinear reaction diffusion equations, and discuss physical implications. In Sect. 3 we define the function $\mathcal{J}(t)$ and use it to determine mathematically how changing the values of the rate constants k_f and k_b affects the chromoamperometric output. In Sect. 4, we present a procedure to extract the rate constants for the reaction from the chronoamperometric output.

[1] For convenience, Figs. 1 and 2 were created with $C_b = 10^{-3}$ mol $\cdot$ cm^{-3} (i.e. 1 **M**). Experimentally, it is necessary to restrict C_b to about 10^{-5} mol $\cdot$ cm^{-3} in order to preserve the requirement that diffusion is the sole mode of mass transport. If C_b is sufficiently small (on the order of 10^{-5} mol $\cdot$ cm^{-3} or lower, generally), then due to various numerical errors, the numerical solver pdepe used above gives results that are too inaccurate to be useful; however, we can scale the given PDEs to a similar set of PDEs with more manageable parameters. If desired, several such scalings (to a variety of different parameters) can be performed; all should result in approximately the same value.

2 Mathematical model

We model Reaction 1 followed by 6 by the following reaction-diffusion system on $(x, t) \in [0, \infty) \times [0, \tau]$, where τ is the duration of the potential step. The $k_f OR$ term is a consequence of the reaction between O and R being first order in each, and the term $k_b P$ is due to P decomposing by first order kinetics. Here, D_O, D_R, and D_P are diffusion coefficients, which in the $k_f > 0$ case we will assume satisfy $D_O = D_R$. This is a physically reasonable assumption since R is created by nothing more than an electron transfer.

$$\begin{cases} \dfrac{\partial O}{\partial t} = D_O \dfrac{\partial^2 O}{\partial x^2} - k_f OR + k_b P \\ \dfrac{\partial R}{\partial t} = D_R \dfrac{\partial^2 R}{\partial x^2} - k_f OR + k_b P \\ \dfrac{\partial P}{\partial t} = D_P \dfrac{\partial^2 P}{\partial x^2} + k_f OR - k_b P \end{cases} \tag{9}$$

with boundary conditions

$$\begin{cases} O(0,t) = 0 \\ R(0,t) = C_b \\ \dfrac{\partial P}{\partial x}(0,t) = 0 \end{cases} \quad \text{and} \quad \begin{cases} \lim_{x\to\infty} O(x,t) = C_b \\ \lim_{x\to\infty} R(x,t) = 0 \\ \lim_{x\to\infty} P(x,t) = 0 \end{cases} \tag{10}$$

and initial conditions

$$\begin{cases} O(x,0) = \begin{cases} 0 & x = 0 \\ C_b & x > 0 \end{cases} \\ R(x,0) = \begin{cases} C_b & x = 0 \\ 0 & x > 0 \end{cases} \\ P(x,0) = 0. \end{cases} \tag{11}$$

This is a system of semilinear reaction-diffusion equations on a half-line[2] with a jump discontinuity in the initial conditions and mixed Neumann and Dirichlet boundary

[2] Throughout this paper, all figures are generated by MATLAB. In order to use it to generate these plots, solutions must be defined on a bounded set. To handle this, we replace the infinite right boundary $x = \infty$ with a large enough finite boundary $x = \hat{x}$. To determine how large $\hat{x}$ must be, we approximate a general $O(x, t)$ for any rate constants k_f, k_b with a simpler function, namely the solution $O_{0,0}(x, t)$ of Eqs. 9–11 if $k_f = k_b = 0$. In that case, the solution of Eqs. 9–11 is $O_{0,0}(x, t) = C_b \mathrm{erf} \frac{x}{\sqrt{4D_O t}}$.Then for any fixed x, $O_{0,0}(x, t)$ decreases with t, since $\mathrm{erf}(z)$ increases with z. If we redefine the right boundary to be at $x = \hat{x}$, then the boundary condition there ($O(\hat{x}, t) = C_b$) will be at its least accurate for the largest t. So if we want the boundary condition to be accurate to 0.01%, then we have to find the $\hat{x}$ for which $O_{0,0}(\hat{x}, \tau) = 0.9999C_b$, which gives $\hat{x} = 5.502\sqrt{D_O \tau}$.

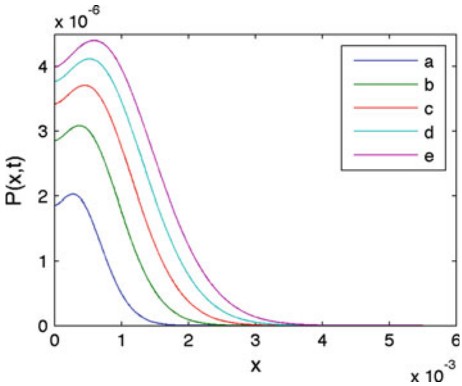

Fig. 3 Concentration profile of reaction product P ($\mathrm{mol} \cdot \mathrm{cm}^{-3}$) with x in cm. $C_b = 10^{-5}\ \mathrm{mol} \cdot \mathrm{cm}^{-3}$, $k_f = 10^7\ \mathrm{cm}^3 \cdot \mathrm{mol}^{-1} \cdot \mathrm{s}^{-1}$ and $k_b = 10\ \mathrm{s}^{-1}$. Here 'a,' 'b,' 'c,' 'd,' and 'e' correspond to fixed times of $t = 0.02, 0.04, 0.06, 0.08, 0.1$, all in s

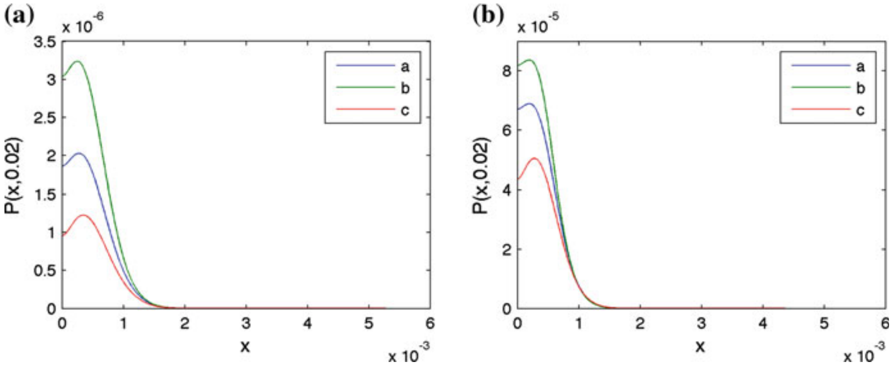

Fig. 4 Concentration profile of the reaction product P ($\mathrm{mol} \cdot \mathrm{cm}^{-3}$) with $D_O = D_R = 2D_P = 10^{-5}\ \mathrm{cm}^2 \cdot \mathrm{s}^{-1}$ throughout. In **a**, $C_b = 10^{-5}\ \mathrm{mol} \cdot \mathrm{cm}^{-3}$ and in **b**, $C_b = 10^{-4}\ \mathrm{mol} \cdot \mathrm{cm}^{-3}$. In both parts, 'a' corresponds to $k_f = 10^7$, $k_b = 10$, 'b' corresponds to $k_f = 2 \times 10^7$, $k_b = 10$, and 'c' corresponds to $k_f = 10^7$, $k_b = 100$, all with k_f expressed in $\mathrm{cm}^3 \cdot \mathrm{mol}^{-1} \cdot \mathrm{s}^{-1}$ and k_b in s^{-1}

conditions. It can be proved that O, R, and P remain bounded in the case $k_b = 0$, and we assume the same result in the general case $k_b > 0$; this is obvious physically due to conservation of mass. Based on results for similar semilinear parabolic systems (e.g. Theorem 2 on page 500 [10]), short term existence and uniqueness is then a reasonable assumption.

This model predicts the expected physical behavior of O, R, and P. To illustrate this, we consider the profile of $P(x, t)$ and how it is affected by the rate constants. In Fig. 3, $P(x, t)$ is shown to reach a maximum near the electrode, but not at $x = 0$. This is logical because the rate of production of P is given by $k_f OR$ and at $x = 0$, $O = 0$, and as $x \to \infty$, $R \to 0$. Furthermore, $P(0, t)$ for $t > 0$ is not zero because P can diffuse back to the electrode surface from the "reaction zone" where the production of P is substantial. Also Fig. 4 shows the predictable effects of C_b, k_f and k_b on $P(x, t)$. Looking, for example, at various times, P increases at the electrode with increasing C_b and increasing k_f but decreases with k_b as it should given that O and R will increase with C_b and that $\frac{dP}{dt} = k_f OR - k_b P$.

3 Theoretical results

We now examine the effect that changing k_f and k_b has on the corresponding current density, so that given a current density we can compare two guessed values of k_f and k_b and determine which is more accurate. When $k_f = k_b = 0$, the solution of the system can be found explicitly, as described in Sect. 3.1. For $k_f > 0$, $k_b = 0$ the key results are in Sect. 3.2, and are the following:

1. Bound O and R using the solution of $O - R$, which we can find explicitly.
2. Using scaling arguments and the maximum principle, prove that our model implies the expected physical behavior: as k_f increases (resp. decreases), $\mathcal{J}$ decreases (resp. increases).

Results for the case $k_f > 0$, $k_b > 0$ are similar to those in Sect. 3.2, and are found in Sect. 3.3.

In what follows, we define $\mathcal{J}(t) := j(t)\sqrt{t}$, and to a current density $j_1(t)$, $j_2(t)$, or $\overline{j}(t)$, denote the corresponding $\mathcal{J}$ by $\mathcal{J}_1$, $\mathcal{J}_2$, and $\overline{\mathcal{J}}$. Similarly, let j_1 be the current density corresponding to a concentration $O_1(x, t)$, etc. We assume throughout that unique solutions exist for Eqs. 9–11. This is an unnecessary assumption only in Sect. 3.1 below, given that in that case we can construct explicit solutions that can be proven to be unique by standard methods.

3.1 $k_f = k_b = 0$

Assume that $k_f = k_b = 0$. Then both the reaction terms $k_f OR$ and $k_b P$ terms are dropped from Eq. 9, which yields the heat equation for each of O, R, and P. These can be solved explicitly, and specifically, $O(x, t) = C_b \mathrm{erf}(x/\sqrt{4D_O t})$. By direct evaluation, this leads to the Cottrell equation, (8). Therefore $\mathcal{J}$ takes on a constant value for all t. As will be seen in the next two sections, this is unique to the $k_f = k_b = 0$ case, and consequently characterizes it: if an experimental $\mathcal{J}(t)$ versus t plot is produced and is seen to be constant, we can deduce without any further calculations that both rate constants are zero.

3.2 $k_f > 0, k_b = 0$

Now assume that $k_f > 0$ and $k_b = 0$, so that the partial differential equations are of the form

$$\begin{cases} \dfrac{\partial O}{\partial t} = D_O \dfrac{\partial^2 O}{\partial x^2} - k_f OR \\ \dfrac{\partial R}{\partial t} = D_O \dfrac{\partial^2 R}{\partial x^2} - k_f OR, \end{cases} \tag{12}$$

the PDE in P being ignored since $k_b P = 0$, to the effect that $P(x, t)$ has no effect on the values of $O(x, t)$ and $\mathcal{J}(t)$. Recall that we are assuming $D_O = D_R$. The boundary and initial conditions are again given by Eqs. 10 and 11.

Lemma 1 is used in the proof of Lemma 2:

Lemma 1 *If O and R solve* (12), (10), (11), *then* $0 \leq O(x,t) \leq C_b \mathrm{erf}\frac{x}{\sqrt{4D_O t}}$ *and* $0 \leq R(x,t) \leq C_b \mathrm{erfc}\frac{x}{\sqrt{4D_O t}}$.

Proof Define $f := O - R (= 2C_b \mathrm{erf}\frac{x}{\sqrt{4D_O t}} - C_b)$ and rewrite the first PDE,

$$L[O] := D_O \frac{\partial^2 O}{\partial x^2} - k_f O(O - f) - \frac{\partial O}{\partial t} = 0,$$

taking O as a solution of the PDE using the usual boundary and initial conditions. Define $u := C_b \mathrm{erf}\frac{x}{\sqrt{4D_0 t}}$. Then

$$L[u] \leq L[O] \leq L[0],$$

as can be checked by direct substitution , and $0 \leq O \leq u$ on the boundary of the domain. By Theorem 12 in Section 3.7 in [12], $0 \leq O \leq u$ everywhere in the domain, as long as L is parabolic with respect to both θO and $\theta O + (1-\theta)u$ for $0 \leq \theta \leq 1$. So we can take $0 \leq O(x,t) \leq C_b \mathrm{erf}\frac{x}{\sqrt{4D_O t}}$. The same argument can be used on the second PDE

$$L[R] := D_O \frac{\partial^2 R}{\partial x^2} - k_f (f + R) R - \frac{\partial R}{\partial t} = 0,$$

instead taking $u := C_b \mathrm{erfc}\frac{x}{\sqrt{4D_O t}}$ to show that $0 \leq R(x,t) \leq C_b \mathrm{erfc}\frac{x}{\sqrt{4D_O t}}$. □

The following two lemmas describe how $\mathcal{J}$ is affected by changing k_f: Lemma 2 says that increasing k_f decreases $\mathcal{J}$ for all t, while decreasing k_f increases $\mathcal{J}$ everywhere. Lemma 3 describes how changing k_f scales $\mathcal{J}$ horizontally. Using these lemmas it can be shown that $\mathcal{J}$ decreases for all t.

Lemma 2 *If $O(x,t) = O_1(x,t)$ and $R(x,t) = R_1(x,t)$ solve* (12), (10), (11) *for $k_f = k_{f1} > 0$ and some bulk concentration C_b, and if $O(x,t) = O_2(x,t)$ and $R(x,t) = R_2(x,t)$ solve* (12), (10), (11) *for $k_f = k_{f2} > 0$ and the same bulk concentration C_b, then $k_{f2} > k_{f1}$ implies $j_1(t) \geq j_2(t)$ and $k_{f1} > k_{f2}$ implies $j_1(t) \leq j_2(t)$.*

Proof Subtracting the equations in Eq. 12, we obtain a linear heat equation in $O - R$, which can be explicitly solved to show that

$$O - R = 2C_b \mathrm{erf}\frac{x}{\sqrt{4D_O t}} - C_b.$$

This is true for any choice of k_f, so define $f(x,t) := O - R$ as given above. Let $O_1,\ O_2,\ R_1$, and R_2 satisfy the suppositions given in the lemma. Then the differential equations can be rewritten as

$$\frac{\partial O_1}{\partial t} - D_O \frac{\partial^2 O_1}{\partial x^2} = -k_{f1} O_1 (O_1 - f) \quad \text{and} \quad \frac{\partial O_2}{\partial t} - D_O \frac{\partial^2 D_O}{\partial x^2} = -k_{f2} O_2 (O_2 - f).$$

Subtracting equations and defining $\widehat{O} := O_1 - O_2$,

$$\frac{\partial \widehat{O}}{\partial t} - D_O \frac{\partial^2 \widehat{O}}{\partial x^2} = k_{f2} O_2 (O_2 - f) - k_{f1} O_1 (O_1 - f)$$

But note that the right hand side can be factored:

$$\begin{aligned} k_{f2} O_2 (O_2 - f) - k_{f1} O_1 (O_1 - f) &= k_{f1}(O_2 - O_1)(O_2 + O_1 - f) \\ &\quad + (k_{f2} - k_{f1}) O_2 (O_2 - f) \\ &= -k_{f1} \widehat{O}(O_2 + R_1) + (k_{f2} - k_{f1}) O_2 R_2. \end{aligned}$$

Therefore

$$\frac{\partial \widehat{O}}{\partial t} - D_O \frac{\partial^2 \widehat{O}}{\partial x^2} + k_{f1} \widehat{O}(O_2 + R_1) = (k_{f2} - k_{f1}) O_2 R_2.$$

Since $O_2, R_1, R_2 \geq 0$, we have $O_2 + R_1 \geq 0$ and $O_2 R_2 \geq 0$ everywhere. Then by the maximum principle, if $k_{f2} - k_{f1} > 0$, then $\widehat{O}(x,t) \geq 0$ everywhere or, equivalently, $O_1(x,t) \geq O_2(x,t)$ [10]. But since $O_1(0,t) = O_2(0,t) = 0$, this implies an inequality for the derivatives as well, as follows:

$$\frac{\partial O_1}{\partial x}(0,t) = \lim_{h \to 0^+} \frac{O_1(h,t)}{h} \quad \text{and} \quad \frac{\partial O_2}{\partial x}(0,t) = \lim_{h \to 0^+} \frac{O_2(h,t)}{h}.$$

If both limits exist, then

$$\frac{\partial O_1}{\partial x}(0,t) - \frac{\partial O_2}{\partial x}(0,t) = \lim_{h \to 0^+} \frac{O_1(h,t) - O_2(h,t)}{h}.$$

Since the expression inside the limit is nonnegative, the limit is as well, from which it follows that

$$\frac{\partial O_1(0,t)}{\partial x} \geq \frac{\partial O_2(0,t)}{\partial x}.$$

Now

$$\left.\frac{\partial O_1}{\partial x}\right|_{x=0} \geq \left.\frac{\partial O_2}{\partial x}\right|_{x=0} \implies j_1(t) \geq j_2(t) \implies \mathcal{J}_1(t) \geq \mathcal{J}_2(t).$$

Similarly, if $k_{f2} - k_{f1} < 0$, then $\widehat{O}(x,t) \leq 0$ everywhere and consequently $j_1(t) \leq j_2(t)$, which then implies $\mathcal{J}_1(t) \leq \mathcal{J}_2(t)$. □

Lemma 3 *Suppose that $O(x,t) = O_1(x,t)$ and $R(x,t) = R_1(x,t)$ solve Eqs. 12 and 10, 11 for $k_f = k_{f1}$ and bulk concentration C_b, and that $O(x,t) = O_2(x,t)$ and $R(x,t) = R_2(x,t)$ solve the same equations but with $k_f = k_{f2}$ and bulk concentration C_b. Then $\mathcal{J}_2(t) = \mathcal{J}_1(t \frac{k_{f2}}{k_{f1}})$.*

Proof Let O_1, O_2, R_1, and R_2 satisfy the above suppositions. Define $\xi := x\sqrt{\frac{k_{f2}}{k_{f1}}}$, $\tau := t\frac{k_{f2}}{k_{f1}}$, and $\overline{O}(x,t) := O_1(\xi,\tau)$. Then:

$$\begin{aligned}\frac{\partial \overline{O}(x,t)}{\partial t} &= \frac{\partial O_1(\xi,\tau)}{\partial \tau}\frac{d\tau}{dt}\\ &= \left(D_O\frac{\partial^2 O_1(\xi,\tau)}{\partial \xi^2} - k_{f1}O_1(\xi,\tau)R_1(\xi,\tau)\right)\frac{k_{f2}}{k_{f1}}\\ &= D_O\frac{\partial^2\overline{O}(x,t)}{\partial x^2} - k_{f2}\overline{O}(x,t)\overline{R}(x,t)\end{aligned}$$

and similarly

$$\frac{\partial \overline{R}}{\partial t} = D_O\frac{\partial^2\overline{R}}{\partial x^2} - k_{f2}\overline{OR}.$$

The boundary conditions are also conserved by the transformations, since $\overline{O}(0,t) = O_1(0,\tau) = 0$, $\overline{R}(0,t) = R_1(0,\tau) = C_b$, $\overline{O}(\infty,t) = O_1(\infty,\tau) = C_b$, and $\overline{R}(\infty,t) = R_1(\infty,\tau) = 0$. Initial conditions are also the same, since $\overline{O}(x,0) = O_1(\xi,0) = O(x,0)$ and $\overline{R}(x,0) = R_1(\xi,0) = R(x,0)$. Therefore $\overline{O}(x,t)$ solves Eqs. 12, 10, 11 and therefore $O_2(x,t) = \overline{O}(x,t) \equiv O_1(\xi,\tau)$. Then

$$\begin{aligned}j_2(t) = nFD_O\left.\frac{\partial O_2(x,t)}{\partial x}\right|_{x=0} &= nFAD_O\left.\frac{\partial O_1(\xi,\tau)}{\partial x}\right|_{x=0}\\ &= nFD_O\left.\frac{\partial O_1(\xi,\tau)}{\partial \xi}\right|_{\xi=0}\frac{d\xi}{dx} = j_1(\tau)\sqrt{\frac{k_{f2}}{k_{f1}}}\end{aligned}$$

and then

$$\mathcal{J}_2(t) = j_2(t)\sqrt{t} = j_1(\tau)\sqrt{t\frac{k_{f2}}{k_{f1}}} = \mathcal{J}_1(\tau),$$

proving the lemma. □

Now we can prove that $\mathcal{J}$ is a decreasing function.

Theorem 1 *If $\mathcal{J}(t)$ corresponds to functions solving Eqs.* 12, 10, 11 *with $k_f = k_{f1} > 0$, then $\mathcal{J}(t)$ decreases with t.*

Proof Let $k_{f2} > k_{f1}$ and let $\mathcal{J}_i(t)$, $i = 1, 2$ correspond to the solution of (12), (10), (11) with $k_f = k_{fi}$. Then by Lemma 3, $\mathcal{J}_2(t) = \mathcal{J}_1\left(t\frac{k_{f2}}{k_{f1}}\right)$ and by Lemma 2, $\mathcal{J}_2(t) \le \mathcal{J}_1(t)$. Therefore

$$\mathcal{J}_1\left(t\frac{k_{f2}}{k_{f1}}\right) \le \mathcal{J}_1(t).$$

Since this is true for any $k_{f2} > k_{f1}$, the above inequality can be rewritten as $\mathcal{J}_1(T) \leq \mathcal{J}_1(t)$ for all $T \geq t$. $\square$

Since $O(x, t) \geq 0$ for all (x, t), it follows that $\mathcal{J}(t) \geq 0$ for all t as well.[3]

3.3 $k_f > 0$ and $k_b > 0$

Here there exists an extra factor $k_b P$ in the partial differential equations that complicates the shape of $\mathcal{J}$. To address this, we make the following assumption:

Assumption 1 If O_1, R_1, P_1 solve Eqs. 9–11 for $k_f = k_{f1}$ and a certain k_b and O_2, R_2, P_2 solve Eqs. 9–11 for $k_f = k_{f2}$ and the same k_b, then $O_1(x, t) \geq O_2(x, t)$ if $k_{f1} < k_{f2}$ and $O_1(x, t) \leq O_2(x, t)$ if $k_{f1} > k_{f2}$.

From a physical perspective, this is a legitimate assumption to make: if O_2 and R_2 are used up faster to make P_2 than O_1 and R_1 are used to make P_1, then we should expect that O_2 will be less than O_1 for all (x, t). The consequence of this assumption is that $\mathcal{J}_1 \geq \mathcal{J}_2$ if $k_{f1} < k_{f2}$ and $\mathcal{J}_1 \leq \mathcal{J}_2$ if $k_{f1} > k_{f2}$.

We can also adapt Lemma 3 to this case; the proof for the following lemma is nearly identical to the proof for Lemma 3. We state only the result:

Lemma 4 *If $\mathcal{J}_1$ corresponds to $k_f = k_{f1}$ and $k_b = k_{b1}$ and $\mathcal{J}_2$ corresponds to $k_f = \kappa k_{f1}$ and $k_b = \kappa k_{b1}$ for some $\kappa > 0$, then $\mathcal{J}_1(\kappa t) = \mathcal{J}_2(t)$.*

Although the assumption and Lemma 4 are almost direct analogues of Lemmas 2 and 3, they cannot be combined into something resembling Theorem 1, since the proof of that theorem depended upon our ability to scale k_f back to its original value after adding or subtracting something from it, which we cannot do here: if we keep k_b constant and change k_f, the new system cannot be scaled back to the system with rate constants k_f and k_b, since the new rate constant ratio is different. In this case, based on the evidence in the case $k_f > 0$, $k_b = 0$, as well as numerical investigations, we assume, without proof, that the minimum exists.

The result of this section can be summarized as follows: keeping k_b constant but increasing k_f will lower the minimum value of $\mathcal{J}$, and by Lemma 4, keeping k_f/k_b constant but varying k_b (or, equivalently, k_f) will shift the minimum point of $\mathcal{J}$ horizontally by a scale determined by the variation of k_b.

4 Procedure to determine k_f and k_b

Suppose that we are given an experimentally determined $\mathcal{J}(t)$, the bulk concentration C_b, and the diffusion coefficients D_O, D_R, and D_P. Here we outline the algorithm to find k_f and k_b:

[3] We can in fact show the stronger result that $\lim_{t\to\infty} \mathcal{J}(t) = 0$, under the additional assumption that if $\lim_{t\to\infty} O(x, t)$ exists, then its derivative is smooth. Since parabolic equations are smoothing and we are considering bounded solutions, this is a good assumption.

1. If for all t, the function $\mathcal{J}(t)$ is constant, then $k_f = 0$ and k_b cannot be determined mathematically, since $P = 0$ and so $k_b P = 0$. However, chemically speaking, given a forward rate constant of zero, the only reasonable backward rate constant is also zero. We therefore take $k_f = k_b = 0$ in this case.
2. If $\mathcal{J}(t)$ is a decreasing function, then $k_b = 0$. To determine k_f, first guess a value; denote this by $k_{f'}$. Numerically evaluate the current density given this rate constant (e.g. using `pdepe` followed by `pdeval` in MATLAB), and denote this by $\overline{\mathcal{J}}(t)$. According to Lemma 3,

$$\mathcal{J}(t) = \overline{\mathcal{J}}\left(t\frac{k_f}{k_{f'}}\right)$$

   Since $\mathcal{J}$ and $\overline{\mathcal{J}}$ are known on a mesh of points t, k_f can be determined directly from the horizontal scaling factor $k_f/k_{f'}$; this can be done for any number of points on the curve.
3. If $\mathcal{J}$ reaches a minimum J at some finite time, then k_f and k_b are both positive. To determine the rate constants, first we determine the rate constant ratio: we make an arbitrary guess of k_b and k_f/k_b and generate the corresponding $\mathcal{J}$; if the minimum of this curve is greater than J, then our guess of k_f/k_b was too low, and if instead the minimum is less than J, then our guess of k_f/k_b was too high. Adjusting the guessed value of k_f/k_b appropriately, we can narrow in on the correct value to any desired degree of accuracy.
   Second, take that ratio together with any k'_b and compute the corresponding $\mathcal{J}$. Let t_m be the time of the minimum of the experimentally determined $\mathcal{J}$ and let t'_m be the time of the minimum of the newly generated $\mathcal{J}$. Due to Lemma 4, $k_b = k'_b t'_m/t_m$. Then since k_f/k_b and k_b are both known, both rate constants are known as well.

If the actual time of the minimum of $\mathcal{J}$, t_m, is misreported as being at a time T_m then the corresponding rate constants satisfy $\frac{k'_f}{k_f} = \frac{t_m}{T_m} = \frac{k'_b}{k_b}$, so the procedure is robust with respect to horizontal translation. Vertical translation is more complicated mathematically, but preliminary results indicate robustness in this direction as well.

To illustrate how the procedure works, suppose that we are given the chronoamperometric data necessary to create Fig. 5. Recall that $\mathcal{J}(t) = j(t)\sqrt{t}$, and $j(t) = i(t)/A$, where $i(t)$ is the raw chronoamperometric data and A is the area of the electrode in cm^2. In all future calculations, we take our units to be as in Fig. 5.

From this plot and C_b and D_O which are taken as 0.00100 mol $\cdot$ cm^{-3} and 10^{-5} cm$^2 \cdot$ s^{-1}, respectively, k_f and k_b can be calculated as follows:

Clearly $\mathcal{J}$ is not constant and is not decreasing everywhere, in contradiction to the results of Sects. 3.1 and 3.2; by elimination it is clear that k_f and k_b are both greater than zero. It is an immediate corollary of Lemma 4 that to any pair of rate constants k_f, k_b, the minimum J_{k_f,k_b} of the corresponding $\mathcal{J}$ depends only on k_f/k_b. Furthermore, it follows from the Assumption in Sect. 3.3 that if k'_f, k'_b are another pair of rate constants with $k'_f/k'_b > k_f/k_b$, then $J_{k_f,k_b} > J_{k'_f,k'_b}$. It is due to this that the value of the minimum alone (here 0.1152) is sufficient to determine k_f/k_b. This

Fig. 5 $\mathcal{J}(t)$ with $C_b = 10^{-3}$ mol $\cdot$ cm^{-3} and $D_O = D_R = 2D_P = 10^{-5}$ cm$^2 \cdot$ s^{-1}. The minimum is at (0.0052, 0.1152)

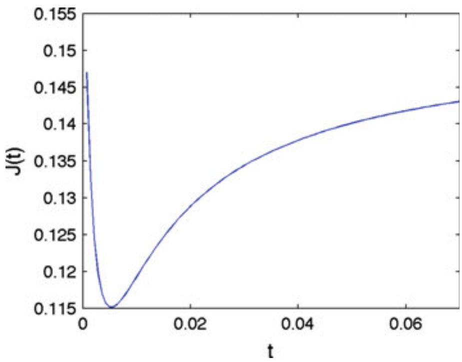

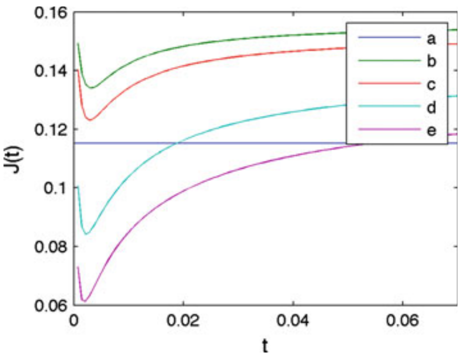

Fig. 6 Here 'a' does not denote any particular $\mathcal{J}(t)$ but rather the experimental minimum 0.1152. Curves 'b'–'e' represent $\mathcal{J}(t)$ versus t for various values of k_f/k_b: 'b' corresponds to $k_f/k_b = 2,000$; 'c' corresponds to $k_f/k_b = 3,000$; 'd' corresponds to $k_f/k_b = 1,0000$; 'e' corresponds to $k_f/k_b = 20,000$. Each curve was generated by $k_b = 500$ and k_f so as to make k_f/k_b the given value; however, as discussed above, these particular values are unimportant at this stage of the calculations

concept is illustrated in Fig. 6; as can be seen, $3{,}000 < k_f/k_b < 10,000$. This method can be continued to any desired degree of accuracy. In particular, here we find that $3,906 < k_f/k_b < 3,922$, and so we approximate $k_f/k_b = 3{,}914$. By choosing each guess based on the bisection method[4], we note that the sequence of guesses converges to the correct answer precisely at the rate of the bisection method.

Next, we guess $k_b = 500$; by calculating the scale to which this guess is incorrect we can approximate the actual value of k_b. The $\mathcal{J}(t)$ corresponding to the choice of $k_f/k_b = 3,914$ and $k_b = 500$ is shown as 'b' in Fig. 7.

As in Fig. 5, 'a' reaches its minimum at $t = 0.0052$, and it can be seen that 'b' reaches its minimum at $t = 0.0027$. As a consequence of Lemma 4, it follows that our guess of $k_b = 500$ was too large by a factor of $\frac{0.0052}{0.0027} = 1.923$. Consequently we calculate $k_b = \frac{500}{1.923} = 260$, which together with $k_f/k_b = 3,914$ implies $k_f = 1.018 \times 10^6$.

[4] i.e. by taking the previous tightest bounds found and letting the new guess be their average; e.g. given $3,000 < k_f/k_b < 10,000$, the next guess would be $k_f/k_b = 6,500$.

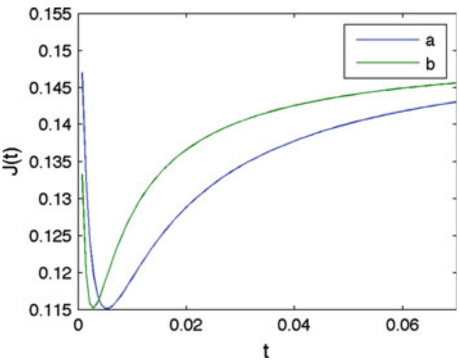

Fig. 7 Here 'a' is the curve from Fig. 5, and 'b' is the $\mathcal{J}(t)$ generated from $k_f/k_b = 3,914$ and $k_b = 500$

Had $\mathcal{J}(t)$ shown no minimum, we note that the computations required in Case 2 are almost identical to the final calculations above.

5 Conclusion

In summary, we have presented a semilinear reaction-diffusion system that models the electrochemical mechanism in which an electrochemical product R consumes the electrochemical reactant O to produce an inactive product P. We introduced a novel method of analyzing chronoamperometric data, by defining and studying the function $\mathcal{J}(t) = j(t)\sqrt{t}$; analytical results are proven for the model using scaling and maximum principle arguments. We then developed an iterative procedure to determine the rate constants from chronoamperometric data.

References

1. W.M. Schwarz, I. Shain, J. Phys. Chem. **69**, 30–40 (1965)
2. J.H. Christie, J. Electroanal. Chem. **13**, 79–89 (1967)
3. D.H. Evans, T.W. Rosanske, P.J. Jiménez, Electroanal. Chem. Interfacial Electrochem. **51**, 449–451 (1974)
4. J.D.E. McIntyre, J. Phys. Chem. **71**, 1196–1207 (1967)
5. T.H. Ridgway, R.P. Van Duyne, C.N. Reilley, J. Electroanal. Chem. **67**, 1–10 (1976)
6. M.L. Olmstead, R.S. Nicholson, Anal. Chem. **41**, 851–852 (1969)
7. C.L. Gardner, D.T. Fouchard, W.R. Fawcett, J. Electrochem. Soc. **128**, 2345–2350 (1981)
8. D. Knittel, J. Electroanal. Chem. **195**, 345–356 (1985)
9. F.C. Laman, C.L. Gardner, D.T. Fouchard, J. Phys. Chem. **86**, 3130–3134 (1982)
10. L.C. Evans, *Partial Differential Equations* (American Mathematical Society, Providence, 1998), p. 500
11. F.G. Cottrell, Z. Physik Chem. **42**, 385 (1902)
12. M.H. Protter, H.F. Weinberger, *Maximum Principles in Differential Equations* (Prentice-Hall, NJ, 1967), pp. 187–190